Fermi National Accelerator Laboratory

FN-464

Longitudinal Coupled-Bunch Instability in the Fermilab Booster*

King-Yuen Ng
Fermi National Accelerator Laboratory
P.O. Box 500, Batavia, Illinois 60510

September 1987

*Talk given at KEK, Tsukuba, Japan, and at the Institute of High Energy Physics of China, Beijing, China, September 1987

Operated by Universities Research Association Inc. under contract with the United States Department of Energy

LONGITUDINAL COUPLED-BUNCH INSTABILITY IN THE FERMILAB BOOSTER*

King-Yuen Ng

KEK National Laboratory for High Energy Physics, Oho-Machi, Tsukuba-Gun, Ibaraki-Ken, 305 Japan

and

Fermi National Accelerator Laboratory, Batavia, IL 60510, U.S.A.

CONTENTS

*Talk given at KEK of Japan and the Institute of High Energy Physics of China, 1987.

I. INTRODUCTION

In this talk, the longitudinal coupled-bunch instability observed in the Fermilab Booster is reviewed and various suggested attempts to cure it are examined.

As you know, the Fermilab Booster and Main Ring were originally built for fixed-target experiments. Therefore, we did not care very much about the individual bunch area formerly. Now, both the Booster and Main Ring become parts of the TEV I project which is a $p - \bar{p}$ collider. About 10 bunches have to be coalesced in the Main Ring to produce a very intense proton or anti-proton bunch to be injected into the Tevatron ring in order to obtain high luminosity. It was discovered that the areas of the individual bunches were to big in the Main Ring so that the coalescence actually lost a significant amount of particles and, as a result, led to the reduction of luminosity in the collider. In the Section II, we go over some experiments that show a growth of bunch area in the Booster due to longitudinal coupled-bunch instability. In Section III, the some important points concerning the theory of coupled-bunch instability are reviewed. In Section IV, a few methods to cure the instability are discussed.

II. GROWTH OF LONGITUDINAL BUNCH AREA

The bunch length of a typical bunch in the Booster across transition had been measured by Crisp.[1] The bunch area was inferred from the rf potential and is shown in Fig. 1. We see that the bunch area is roughly constant before transition but increases abruptly afterward. The mountain-range plot of Fig. 2a reveals quadrupole oscillations of the bunch after transition. This is due to space-charge effects[2] which alter the rf potential and allow for a longer (shorter) bunch before (after) transition as shown in Fig. 3. Thus, after transition, the bunch does not fit the bucket and starts tumbling (Fig. 4). A transition-jump mechanism was later installed and Fig. 2b shows the new mountain-range plot. With the elimination of the space-charge effects, we begin to see a coupled-bunch pattern.

Some new measurements were performed by Cornacchia and Crisp.[3] The transverse beam size was measured with a flying wire and, at the same time, the bunch length was also measured with the longitudinal pick-up. Figure 5 shows the measured beam half size as a function of time in the acceleration cycle. Four of the 18 rf cavities were disconnected but not shorted. The beam intensity at high energies was 1.5×10^{12} protons for a total of 84 bunches. We observe an increase in beam size at transition (~ 19 sec after injection). We also observe that the horizontal beam size increases at high energies. The measured beam size is compared with the calculated value, obtained by adding quadratically the contribution of the momentum spread and the horizontal emittance. The momentum spread was inferred from the measured bunch length and the known rf parameters, while a normalized transverse emittance of 8π mm-mrad was

assumed. The good agreement between the two curves indicates that, at this intensity, no betatron blow up occurs, and that the longitudinal instability only is responsible for the observed increase in beam size. The half beam size was next measured with the four disconnected cavities shorted and is plotted in Fig. 6. The increase in beam size at high energies was reduced showing that the growth is driven by the rf cavities. The calculated bunch size assuming a constant normalized emittance of 8π mm-mrad and a constant bunch area of 0.025 eV-sec does not agree with the measured value. This demonstrates again that the discrepancy is due to an increase in bunch area at higher energies. Figure 7 shows the bunch area inferred from the measured bunch length as a function of time with four of the rf cavities shorted and also with the cavities unshorted. The growth in bunch area at high energies reveals clearly a longitudinal instability and that the cavities were responsible for the instability. We suspect that this is a longitudinal coupled-bunch instability driven by the parasitic modes of the cavities.

III. LONGITUDINAL COUPLED-BUNCH INSTABILITY

Consider M equal rigid bunches each containing N protons engaging in a coupled-bunch oscillation of mode μ. This means that the synchrotron phase of each bunch lags that of the preceeding bunch by $2\pi\mu/M$. For closure, it is clear that μ must be an integer and can assume M values, which we choose here as 0, 1, $\cdots$, $M-1$. The current is given by

$$I(t) = eN\omega_0 \sum_{\ell=0}^{M-1} \delta_p \left[\omega_0 t - \frac{2\pi\ell}{M} + \epsilon\cos\left(\omega_s t + \frac{2\pi\mu\ell}{M}\right)\right] , \tag{3.1}$$

where ω_0 is the angular frequency of revolution, ω_s the angular synchrotron frequency and ϵ the amplitude of synchrotron oscillation. The delta function δ_p is approximately periodic. Neglecting this approximation, we expand it into harmonics, giving

$$I(t) = \frac{eN\omega_0}{2\pi} \sum_{m=-\infty}^{\infty} \sum_{\ell=0}^{M-1} \exp im \left[\left(\omega_0 t - \frac{2\pi\ell}{M}\right) + \epsilon\cos\left(\omega_s t + \frac{2\pi\mu\ell}{M}\right)\right] .$$

Written in terms of Bessel functions, the summations over ℓ and m can be performed and we get

$$I(t) = \frac{eN\omega_0}{2\pi} \sum_{p=-\infty}^{\infty} \sum_{n=-\infty}^{\infty} (-i)^n J_n[(pM+n\mu)\epsilon] e^{i[(pM+n\mu)\omega_0 + n\omega_s]t} .$$

Here, the $n = 0$ term gives the spectrum of the M uncoupled bunches. The lowest-order coupling comes from $n = 1$ term, which provides a spectrum of

$$I(t) = \frac{eN\omega_0\epsilon}{2\pi} \sum_{p=-\infty}^{\infty} (pM+\mu)\sin[(pM+\mu+\nu_s)\omega_0 t] , \tag{3.2}$$

where $\nu_s = \omega_s/\omega_0$ is the synchrotron tune.

The spectrum given by Eq. (3.2) is plotted in Fig. 8 for the μth and $(M-\mu)$th modes. When the negative-frequency side is folded onto the positive-frequency side as one would take measurement in an experiment, we see that the spectral lines for the μth and $(M-\mu)$th modes are separated by only $2\omega_s/2\pi$ which amounts to $\sim$4 kHz for the Booster and cannot be resolved by the frequency analyzer. For this reason, mode μ and mode $(M-\mu)$ cannot be differentiated.

The frequency shift for the rigid or dipole mode is given by[4]

$$\Delta\nu_s = \frac{ie\eta I_b M}{4\pi\beta^2\nu_s E} Z_{\text{eff}} \ , \tag{3.3}$$

where, for a gaussian bunch of rms length σ_ℓ, the effective impedance is

$$Z_{\text{eff}} = \sum_{p=-\infty}^{\infty} \nu_p e^{-(\nu_p\sigma_\ell/R)^2} Z(\nu_p\omega_0) \ , \tag{3.4}$$

and

$$\nu_p = pM + \mu + \nu_s \ . \tag{3.5}$$

Note that only the spectral lines of Eq. (3.2) contribute in the impedance $Z(\omega)$. In the above, η is the frequency dispersion, β the velocity relative to light velocity, I_b is the average current of one bunch, and R and radius of the Booster ring. As is evident from Eq. (3.3), the real part of the impedance Z contributes an imaginary frequency shift, resulting in a growth for the positive-frequency spectral lines and damping for the negative-frequency spectral lines. When the negative-frequency portion is folded onto the positive-frequency portion, the modes $\mu = 0$ and $\mu = M/2$ if M is even have their growth and damping lines separated by $2\omega_s$ only (Fig. 9). Therefore, if the driving resonance impedance has a width bigger than that, these two modes should be stable.

Figure 10 shows mode 53 or 31 (there are $M = 84$ bunches) excited and Fig. 11 shows the growth of mode 16 or 68. Table I shows 14 resonances of the rf cavities measured by Crisp.[5] The correct shunt impedances and Q's were calculated by taking the known shunt impedance and Q of the fundamental as a reference. These resonances will be crossed by one or more spectral lines as the particle is accelerated and coupled-bunch growth of some modes will be excited. Table II shows the average growth rate of each mode driven by the resonances, the principal one being underlined. However, only two coupled modes were actually observed. We conjecture that only resonances number 2 and 4 have been crossed by the spectral lines therefore exciting modes near 16 and 53. The frequencies of the other resonances increase as the rf cavities are tuned gradually to accommodate higher energies. As a result, these resonances may not be crossed by any spectral lines at all. It was actually observed that resonances number 2 and 4 do not have their frequencies changed during acceleration.

Resonance Number	Frequency (MHz)	Shunt Impedance (MΩ)	Q
1	52.3	0.43	1307
2	85.8	1.56	3380
3	109.7	0.15	2258
4	167.2	0.07	1960
5	171.5	0.07	1190
6	225.4	0.33	2090
7	318.1	0.09	1570
8	342.6	0.50	530
9	391.0	0.11	460
10	448.8	0.48	3590
11	448.8	0.11	1206
12	559.7	0.07	430
13	685.9	0.71	2440

Table I: Measured resonant frequency, shunt impedance, and Q of the Booster accelerating cavities.

IV. WAYS TO CURE THE COUPLED-BUNCH INSTABILITY

Several methods have been suggested to cure the instability. We shall discuss each of them briefly.

1. Damping of the two resonances

One cell of the Booster rf cavities is shown in Fig. 12. By applying suitable voltages across the resistances at the top, the electromagnetic fields inside the cavity cell can be altered. Thus certain modes can be enhanced or diminished. Crisp[6] has analyzed the field structures of these parasitic modes and has been able to apply the suitable voltages to damp down number 2 and 4. This results in a reduction of the the coupled-bunch mode amplitudes to a certain degree but the reduction is not big enough to be really useful.

2. Feedback damper

To cure coupled-bunch effects, the damping must be bunch by bunch and must therefore be fast. The rf frequency is $\sim$ 52 MHz. Thus, the feedback system must have a bandwidth of the order or larger than 26 MHz. If the energy spread ϵ has a growth

Mode μ	Average Growth rate in ms^{-1}	Driving Resonances	Mode μ	Average Growth rate in ms^{-1}	Driving Resonances
0	0.	(13)	34	0.793	(9)
1	0.563	(13)	35	0.618	(9)
2	0.695	(7,**13**)	36	0.506	(9)
3	0.579	(7,**13**)	37	0.429	(9)
4	0.526	(7,**13**)	38	0.371	(9)
5	0.474	(7,**13**)	39	0.326	(9)
6	0.430	(7,**13**)	40	0.288	(9)
7	0.737	(3,7,**13**)	41	3.208	(**8**,9)
8	0.404	(3,7,**13**)	42	0.	(**8**,10,11)
9	0.284	(13)	43	2.344	(**8**,10,11)
10	0.267	(13)	44	2.033	(**8**,10,11)
11	0.252	(13)	45	1.780	(**8**,10,11)
12	0.238	(13)	46	1.548	(**8**,10,11)
13			47	1.382	(**8**,10,11)
14	0.074	(4)	48	0.314	(**10**,11)
15	0.045	(4)	49	0.285	(**10**,11)
16	0.032	(4)	50	0.263	(**10**,11)
17	0.025	(4)	51	0.472	(12)
18			52	1.111	(2,**12**)
19			53	0.568	(2,**12**)
20			54	0.311	(12)
21	0.106	(5)	55	0.279	(12)
22	0.067	(5)	56	0.253	(12)
23	0.372	(5,**6**)	57	0.231	(12)
24	0.269	(5,**6**)	58	0.213	(12)
25	0.179	(6)	59	0.197	(12)
26	0.147	(6)	60	0.184	(12)
27			61	0.172	(12)
.			.		
.			.		
.			83	0.751	(13)

Table II: Average growth rate for each mode μ. When there are more than one responsible driving resonance, the one that contributes mostly is bold-faced.

time τ, the maximum voltage per turn V required by the system is given by

$$eV = \frac{2E\dot{\epsilon}}{f_0} = \frac{2E\epsilon}{\tau f_0} , \tag{4.1}$$

where the revolution frequency f_0 is 0.63 MHz. For a circulating current containing 2.2×10^{12} protons, a worst growth is of the order 0.2 ms at the peak energy of $E =$ 8.9 KeV. If the transverse pick up has the capability of detecting a position error of 0.2 mm at the location where the dispersion is 1.5 m, the minimum detectable energy spread will be 1.3×10^{-4}. Therefore, the minimum voltage per turn required for the feedback system is 19 kV. Such a fast feedback system is under investigation at the moment.

3. Self-excited cavity

The coherent frequency shift or tune shift for coupled-mode μ is given by Eq. (3.3). We have mentioned that any spectral line on the positive-frequency side may drive a growth while any line on the negative-frequency side may drive a damping. Consider coupled-mode 53 in Fig. 14, the spectral line $(84 + 53 + \nu_s)\omega_0$ will cross resonance number 2 during acceleration and this line will receive a growth. For the mode 31, on the other hand, the spectral line $(-2 \times 84 + 31 + \nu_s)\omega_0$ will cross the same resonance at negative frequency and receive a damping. But there are also other negative spectral lines for mode 53, for example, the line $(-2 \times 84 + 53 + \nu_s)\omega_0$. Unfortunately, they do not contribute usually because they will not cross that resonance. However, if we insert in the Booster ring a cavity with frequency $|(-2 \times 84 + 53 + \nu_s)\omega_0|$, the line $(-2 \times 84 + 53 + \nu_s)\omega_0$ will cross it at negative frequency and contribute a damping.[7] With the introduction of this complementary resonance, the line $(84 + 31 + \nu_s)\omega_0$ for mode 31 will cross it at positive frequency and will contribute a growth for this mode. We would like to adjust this complementary cavity so that the growth due to the driving resonance number 2 will be cancelled and the extra growth for mode 31 will be cancelled also. We also would like to have both resonances crossed at the same time so that the dampings will set in as soon as the growths occur. But this is impossible because all the spectral lines are shifted to the right by an amount ω_s. Let the frequency of the original resonance number 2 be $\omega_r = (84+53+\nu_s)\omega_0$, where ω_0 is the angular revolution velocity when the mode 53 spectral line crosses the resonance. If we place the complementary resonance at $\omega_r' = |(-2 \times 84 + 53 + \nu_s)\omega_0|$, the damping and growth of mode 53 will occur at the same time. However, the growth line corresponding to mode 31 will cross the complementary resonance at an earlier time while the negative-frequency damping line will cross the original resonance at a later time. It is nice to choose the position of the complementary resonance to be at

$$\omega_r' = \omega_r \frac{|-p'M + \mu|}{pM + \mu} , \tag{4.2}$$

where p and p' are the integers that correspond to the growth-spectral lines of mode μ and mode $M-\mu$ that cross the original and complementary resonances respectively. In our example, $p=1$, $p'=2$, and the complementary resonance is chosen at $\omega_r'=|(-2\times 84+53)\omega_0|$. In this case, for both mode μ and mode $M-\mu$, the damping will lag the growth by just a small amount of the order

$$\Delta t=\frac{\omega_s E}{\eta\omega_R\omega_0\dot{E}}\ , \tag{4.3}$$

where ω_R is either ω_r or ω_r', η the momentum dispersion, E the particle energy at the crossing of the resonances, and $\dot{E}$ the acceleration at that time.

To obtain a complete damping of the growth and to require the time periods for growth and damping (or the crossing times of the two resonances) to be exactly the same, we have to choose the Q and the shunt impedance of the complementary resonance as

$$Q'=Q\ , \tag{4.4}$$

$$Z_s'=Z_s\frac{pM+\mu+\nu_s}{|-p'M+\mu+\nu_s|}\ . \tag{4.5}$$

We try to add a complementary resonance to resonance number 2 (85.80 MHz) with the parameters:

	f_r (MHz)	Z_s (MΩ)	Q
original	85.80	1.887	3378
complementary	72.02	1.887	3378

according to Eqs. (4.2), (4.4), and (4.5). The growth rates as functions of energy for modes 53 and 31 are shown Fig. 13. We see that in each case the damping comes in slightly after the growth as expected. Also in each case, the damping does not cancel the growth completely. However, the residual growths can be damped by Landau damping.

However, this method will not work for resonance number 4 at $\omega_r/2\pi=167.2$ MHz. The reason is, during the acceleration cycle, resonance number 2 is crossed mainly by mode 53 only (or mode 31 for damping) but resonance number 4 is crossed first by mode 16, then 15 and lastly 14. To cancel mode 16 at the time it is growing, we need only to put a complementary resonance ω_r' (and of course $-\omega_r'$) between spectral lines 15 and 16 of another band as shown in Fig. 14. This resonance, however, will excite dampings of modes 14 and 15 well before their growths are driven by the original resonance. Also, this complementary resonance will excite growth for mode 67 and possibly mode 66, and no damping will be provided for these modes by the original resonance at all. We therefore conclude that the addition of a complementary resonance works only in the situation when the original resonance is crossed by only a spectral line of only one coupled-bunch mode.

4. Higher-harmonic cavity[8]

A higher-harmonic cavity can be introduced to provide a bigger spread in synchrotron frequency and hopefully more Landau damping. The original rf voltage

$$V(\varphi) = V_0 \sin(\varphi + \varphi_s) \tag{4.6}$$

is changed to

$$V(\varphi) = V_0[\sin(\varphi + \varphi_s) + k \sin(m\varphi + m\varphi_m)] \ , \tag{4.7}$$

where kV_0 is the peak voltage of the higher-harmonic cavity with frequency m times that of the rf. To obtain a bigger spread of oscillation frequency, we would like the bottom of the potential well, which is the integral of $V(\varphi)$, to be as flat as possible. There are four parameters: k, m, φ_m, and the constant of integration of $V(\varphi)$. For $\varphi = 0$, we set the potential well to zero and demand

$$V'(\varphi) = 0 \ , \qquad V''(\varphi) = 0 \ . \tag{4.8}$$

We obtain the conditions

$$\cos \varphi_s = -km \cos m\varphi_m \ , \qquad \sin \varphi_s = -km^2 \sin m\varphi_m \ . \tag{4.9}$$

For small φ, the potential well becomes a quartic,

$$\int V(\varphi) \rightarrow \frac{m^2 - 1}{12} \varphi^4 V_0 \cos \varphi_s \ , \tag{4.10}$$

and the synchrotron frequency has a spread proportional to the oscillation amplitude,

$$\frac{\omega_s(\varphi)}{\omega_{s0}} = \frac{\pi}{2} \left(\frac{m^2 - 1}{6} \right)^{1/2} \frac{\varphi}{K_0} \ . \tag{4.11}$$

In the above, ω_{s0} is the synchrotron frequency at zero amplitude (without the higher-harmonic cavity) and $K_0 = 1.854$ is the complete elliptic integral of the first kind with argument 1/2. Although the spread depends on m^2 as is evident from Eq. (4.11), m cannot be too big or the bunch will have variation in density. Our bunch has a rms length of $\sigma_\varphi = 0.16$ rf rad or a half length of $2\sqrt{2}\sigma_\varphi = 0.45$ rf rad. If we want this half length to be within the first dip of the potential due to the term $\cos m\varphi$, the highest harmonic allowed is $m = 4$.

Now let us turn to mode-coupling. For the harmonic (usual) rf cavity, the bunch spectrum shown in Fig. 15 is

$$\nu_p \omega_0 = (pM + \mu + a\nu_s + \Delta\nu_{sa})\omega_0 \ , \tag{4.12}$$

where μ is the couple-mode number and a the single-bunch harmonic mode number. The term $\Delta\nu_{sa}\omega_0$, which can be complex, represents the frequency shift due to the

driving impedance. Since each bunch mode (represented by a) is separated from each other by $\sim \nu_{s0}\omega_0$, for small perturbation $|\Delta\nu_{sa}| \ll \nu_{s0}$, we can consider only one mode and neglect the others. Of course this this not true for high beam current where mode-mixing can occur.

For the higher-harmonic cavity, the frequency of oscillation $\omega_s(\varphi)$ in Eq. (4.11) for all modes (any a) starts from zero for a bunch of vanishing length as shown in Fig. 16 independent of how small the beam current is. This is a highly degenerate situation[9] (like Zeeman effect in quantum mechanics). In doing perturbation, we should have the correct set of orthogonal eigenfunctions to start with so that the reaction matrix is diagonalized. This means that we cannot just take the dipole mode $a = 1$ and forget the others.

If the bunch is short, however, Krinsky and Wang[9] show that, as an approximation, we can take only $a = \pm 1$ and neglect the others. The Vlasov equation then becomes, for $a = \pm 1$,

$$R_a(\Omega) + iA \sum_{a'=\pm 1} a' i^{a-a'} \int_0^\infty \frac{\psi_0'(r) r^2 dr}{\Omega\beta - a\omega_s(r)} R_{a'}(\Omega) = \Phi_a(\Omega) \ . \tag{4.13}$$

In the above, ψ_0 is the unperturbed particle distribution normalized to

$$\int \psi_0(r) d\delta d\varphi = 1 \ , \tag{4.14}$$

with $\delta = \Delta E/E$ the energy spread, φ the phase angle along the Booster ring in rf rad, and $\varphi = r\cos\phi$, $\eta h\delta/\beta^2\nu_{s0} = r\sin\phi$. Also, $R_a(\Omega)$ is the Fourier transform of the perturbed distribution of harmonic a, β is the velocity relative to light velocity c of the particle with energy E, $\Phi_a(\Omega)$ represents some initial condition of the perturbation, Ω is the Fourier-transform frequency, and

$$A = \frac{e^2\omega_0}{8\pi E h^2} Z_{\text{eff}} \ , \tag{4.15}$$

with h (here equal to M) the rf harmonic. The effective impedance Z_{eff} is given by Eq. (3.4), but the power spectrum may be different for different potential well.

We diagonalize the Vlasov equation. One eigenfunction is $R(\Omega) = R_1(\Omega) + R_{-1}(\Omega)$. We solve for $R(\Omega)$ and take the inverse Fourier transform by integrating over Ω. The zeroes of the denominator in the integrand of the inverse transform,

$$H(\Omega) = 1 + iA \int_0^\infty \psi_0'(r) r^2 dr \left(\frac{1}{\Omega\beta - \omega_s(r)} - \frac{1}{\Omega\beta + \omega_s(r)} \right) \tag{4.16}$$

give the solution of the collective frequency Ω, and

$$H(\Omega) = 0 \tag{4.17}$$

is the usual dispersion relation. This relation holds when $\mathcal{I}m\,\Omega > 0$ and it must be continued analytically to the negative $\mathcal{I}m\,\Omega$-half plane according to the method of Landau.

If the cavity is approximately harmonic, the unperturbed particle distribution is

$$\psi_0(r) = \frac{1}{2\pi\sigma_\varphi^2}\left(\frac{\eta h}{\beta^2\nu_{s0}}\right)e^{-r^2/2\sigma_\varphi^2}\ , \tag{4.18}$$

and the spread in synchrotron frequency due to the cosine shape of the potential is

$$\omega_s(r) = \omega_{s0}\left(1 - \frac{r^2}{16}\frac{1-\sin^2\varphi_s}{1-\sin^2\varphi_s}\right)\ . \tag{4.19}$$

Denote the frequency shift by

$$\Delta\Omega\beta = \Omega\beta - \omega_{s0}\ , \tag{4.20}$$

and the mean frequency spread by

$$\delta\omega_s = \frac{\omega_{s0}\sigma_\varphi^2}{8}\ , \tag{4.21}$$

assuming that $\sin\varphi_s \sim 0$. Then, the dispersion relation of Eq. (4.17) becomes ($r = \sqrt{2}\sigma_\varphi x$),

$$1 = i\frac{\eta M I_b\omega_0}{2\pi\beta^2\nu_{s0}E/e}Z_{\rm eff}\int_0^\infty \frac{e^{-x^2}x^3}{\Delta\Omega\beta + \delta\omega_s x^2}dx\ , \tag{4.22}$$

where I_b is the average current of *one* bunch. In Eq. (4.22), only one term of the dispersion relation ($a = +1$) has been included because when $\Omega\beta$ is near to ω_{s0}, it is far away from $-\omega_{s0}$.

When a spectral line in $Z_{\rm eff}$ is at the peak of a sharp resonance, there is a big growth and usually $\mathcal{I}m\,\Delta\Omega \gg \delta\omega_s$. This means that $\Delta\Omega$ can be taken out of the integral sign. The integral can of course be done easily and we get

$$\frac{\mathcal{I}m\,\Delta\Omega\beta}{\omega_0} = \frac{\eta M I_b}{4\pi\beta^2\nu_{s0}E/e}Z_{\rm eff}\ , \tag{4.23}$$

which is exactly the same as Eq. (3.3). Physically this implies the neglect of Landau damping when it is much less than the growth.

Now, for the higher-harmonic cavity, the unperturbed distribution is

$$\psi_0(r) = \frac{\eta^2h^2\omega_0^2}{2\sqrt{\alpha}K_0\beta^6c^2r_0^3\Gamma(3/4)}e^{-(r/r_0)^4}\ , \tag{4.24}$$

where $K_0 = 1.854$ and

$$\alpha = \frac{m^2-1}{4!}\left(\frac{\eta\omega_{s0}h\omega_0}{\beta^4c^2}\right)^2\ .$$

The amplitude-dependent synchrotron frequency obtained from Eq. (4.11) is

$$\omega_s(r) = \frac{\pi\omega_{s0}}{K_0}\sqrt{\frac{m^2-1}{24}}r \ . \tag{4.25}$$

The dispersion relation of Eq. (4.17) becomes (now both $a = +1$ and $a = -1$ terms are needed)

$$1 = iBC_4\int_0^\infty \frac{x^6 e^{-x^4}}{(\Omega\beta)^2 - (\delta\omega_s x)^2}dx \ , \tag{4.26}$$

where $x = r/r_0$ and the mean spread in frequency is

$$\delta\omega_s = \omega_s(r_0) = \frac{\pi\nu_{s0}\sigma_\varphi}{\beta K_0}\sqrt{\left(\frac{m^2-1}{4!}\right)\frac{\Gamma(1/4)}{\Gamma(3/4)}} \ , \tag{4.27}$$

and

$$B = \frac{\eta M I_b\omega_0}{2\pi\beta^2 E/e}Z_{\rm eff} \ , \qquad C_4 = \frac{2\pi^2}{K_0^2\Gamma(3/4)} = 4.68 \ .$$

Again at the top of a resonance, $|\Omega\beta| \gg \delta\omega_s$, we have $\Omega\beta \sim (1+i)\sqrt{B/2}$, or

$$\frac{\mathcal{I}m\,\Omega\beta}{\omega_0} = \sqrt{\frac{\eta M I_b}{4\pi\beta^2 E/e}Z_{\rm eff}} \ . \tag{4.28}$$

By the way, if you have taken only the $a = +1$ term and neglected the other (this is *wrong*), we get instead a dispersion relation

$$1 = i\frac{BC_4}{2\delta\omega_s}\int_0^\infty \frac{x^5 e^{-x^4}}{\Omega\beta - \delta\omega_s x}dx \ . \tag{4.29}$$

At a resonance, when $|\Omega\beta| \gg \delta\omega_s$, we get a growth rate $\mathcal{I}m\,\Omega\beta \sim B/2\delta\omega_s$, or

$$\frac{\mathcal{I}m\,\Omega\beta}{\omega_0} = \frac{\eta M I_b\omega_0}{4\pi\beta^2\delta\omega_s E/e}Z_{\rm eff} \ . \tag{4.30}$$

We see that Eq. (4.23) describing the growth rate with a harmonic cavity is very different from Eq. (4.28) describing the growth rate with a higher-harmonic cavity. Of course, these two expressions are different from Eq. (4.30) when one term has been left out by mistake. Therefore, we cannot tell before hand whether a high-harmonic cavity is better than a harmonic cavity. In fact, if we take resonance number 2, it turns out that the growth rate is bigger for the higher-harmonic cavity. The results are shown in Table III. The last row of the table shows that our assumption of $|\Delta\Omega\beta| \gg \delta\omega_s$ holds in each case. The second last row shows that the neglect of the $a = -1$ mode for the harmonic cavity is still correct, because the separation of the two modes starts with $2\omega_{s0}$.

Input:

Right at the peak of resonance number 2 with

$$f_r = 85.80 \text{ MHz}, \; R_s = 1.564 \text{ M}\Omega, \text{ and } Q = 3378,$$

particle energy is at $E = 6.87$ GeV,

revolution frequency $\omega_0 = 3.939$ MHz,

momentum compaction $= 0.03464$, $\quad \eta = 0.01598$,

rf peak voltage $V_0 = 446$ kV, synchronized phase $\varphi_s = 25°$,

bunch area $= 0.025$ eV-sec (95%),

$M = 84$ bunches with $N = 3.5 \times 10^{10}$ each,

coupled-bunch mode $\mu = 53$,

higher-harmonic cavity has $m = 4$.

Output:

$I_b = 0.00352$ amp/bunch, $\quad \nu_{s0} = 0.00358$.

	Harmonic Cavity	Higher-harmonic Cavity	
		$a = \pm 1$	$a = +1$ (wrong)
σ_ℓ	14.0 cm	17.8 cm	17.8 cm
σ_φ	0.156 rf rad	0.198 rf rad	0.198 rf rad
σ_δ	4.08×10^{-4}	2.40×10^{-4}	2.40×10^{-4}
$\frac{\mathcal{I}m\,\Delta\Omega}{\omega_0}$	0.00327	0.00356	0.00740
$\frac{\lvert\Delta\Omega\rvert}{\omega_{s0}}$	0.914	1.40	2.07
$\frac{\lvert\Delta\Omega\rvert}{\delta\omega_s}$	300	3.05	4.48

Table III: Comparison of maximum growth rate for different cavities driven by resonance number 2.

Exact solution of the dispersion relations of Eqs. (4.22) and (4.26) is shown in Fig. 17. It confirms our former results at the peak of the resonance. The total growth across the resonance for the higher-harmonic cavity, however, is much bigger than that for the harmonic cavity, although the damping which comes in later cancels the growth nearly completely. But a damping which lags the growth by so much may not be of any effect. The same solution for resonance number 4 and coupled-mode $\mu = 16$ is shown in Fig. 18. Here, the growth with the higher-harmonic cavity is definitely much less.

The ratio of the growths in Eqs. (4.22) and (4.26) gives

$$\frac{(\mathcal{I}m\,\Delta\Omega)_{\mathbf{harm}}}{(\mathcal{I}m\,\Omega)_{\mathbf{higher}}} = \sqrt{\frac{\eta M I_b Z_{\mathbf{eff}}}{4\pi\beta^2\nu_{s0}^2 E/e}}\,. \tag{4.31}$$

It appears that if the shunt impedance of the resonance is very big, the growth with a higher-harmonic cavity will be less. However, a higher-harmonic cavity is also more beneficial for a weak resonance peak too. When the driving resonance is weak, the actual growth can be of the same magnitude or even less than the damping effect provided by the cavity, which is the situation for resonance number 4. Therefore damping cannot be neglected. In other words, $\Delta\Omega\beta$ or $\Omega\beta$ cannot be taken out of the integral sign in their respective dispersion relation, Eq. (4.22) or (4.22). As a result, Eq. (4.31) or Eqs. (4.22) and (4.26) do not apply. A higher-harmonic cavity therefore works well for very strong and very weak impedance resonances but not for something in between like resonance number 2. It will definitely help in the case of a broad-band impedance where the growth rate is slow everywhere and is less the Landau damping provided. The physical reason why a higher-harmonic cavity does not work for a medium-size resonance is: the damping, although much bigger than that provided by the usual harmonic cavity, is nevertheless small compared to the growth driven by such a resonance. The damping, however, is the real merit of the higher-harmonic oscillator. Therefore, it is not strange to see the cavity fail its job when damping (or its merit) is neglected.

5. Remarks

For the four methods that we discussed above, it appears that each method has its good points and also its bad points. Damping down the two annouying parasitic modes helps only a little. A fast feedback damper is good but is hard to built. A self-exciting cavity will help damping out resonance number 2 which is crossed by only one coupled mode. It does not work for resonance number 4 which is crossed by several coupled modes. A higher-harmonic cavity works for the weak resonance number 4, but performs poorly for the stronger resonance number 2. Some other methods need consideration; for example, variation in particle number among the bunches or application of an extra rf which is lower than the acceleration rf.

ACKNOWLEGEMENT

Part of this work was done while the author was on leave at KEK National Laboratory for High Energy Physics, Japan. He would like to thank Professor Y. Kimura and the Accelerator Theory Group for the invitation and their hospitality during his stay.

REFERENCES

1. J. Crisp, private communication.
2. K. Y. Ng, Fermilab Report FN-436; A. Sorenseen, Particle Accelerators **6**, 141 (1975).
3. M. Cornacchia, Fermilab Report TM-1442 or LBL-22978.
4. see for example, A. W. Chao, in *Second Summer School on High Energy Particle Accelerators*, SLAC, Stanford, August 1982, Ed. M. Month.
5. J. Crisp, private communication.
6. J. Crisp, private communication.
7. K. Y. Ng, Fermilab Report FN-456; the idea was initiated by J. Griffin.
8. Y. Chao and K. Y. Ng, Fermilab Report (in preparation).
9. S. Krinsky and J. M. Wang, Particle Accelerators **17**, 109 (1985).

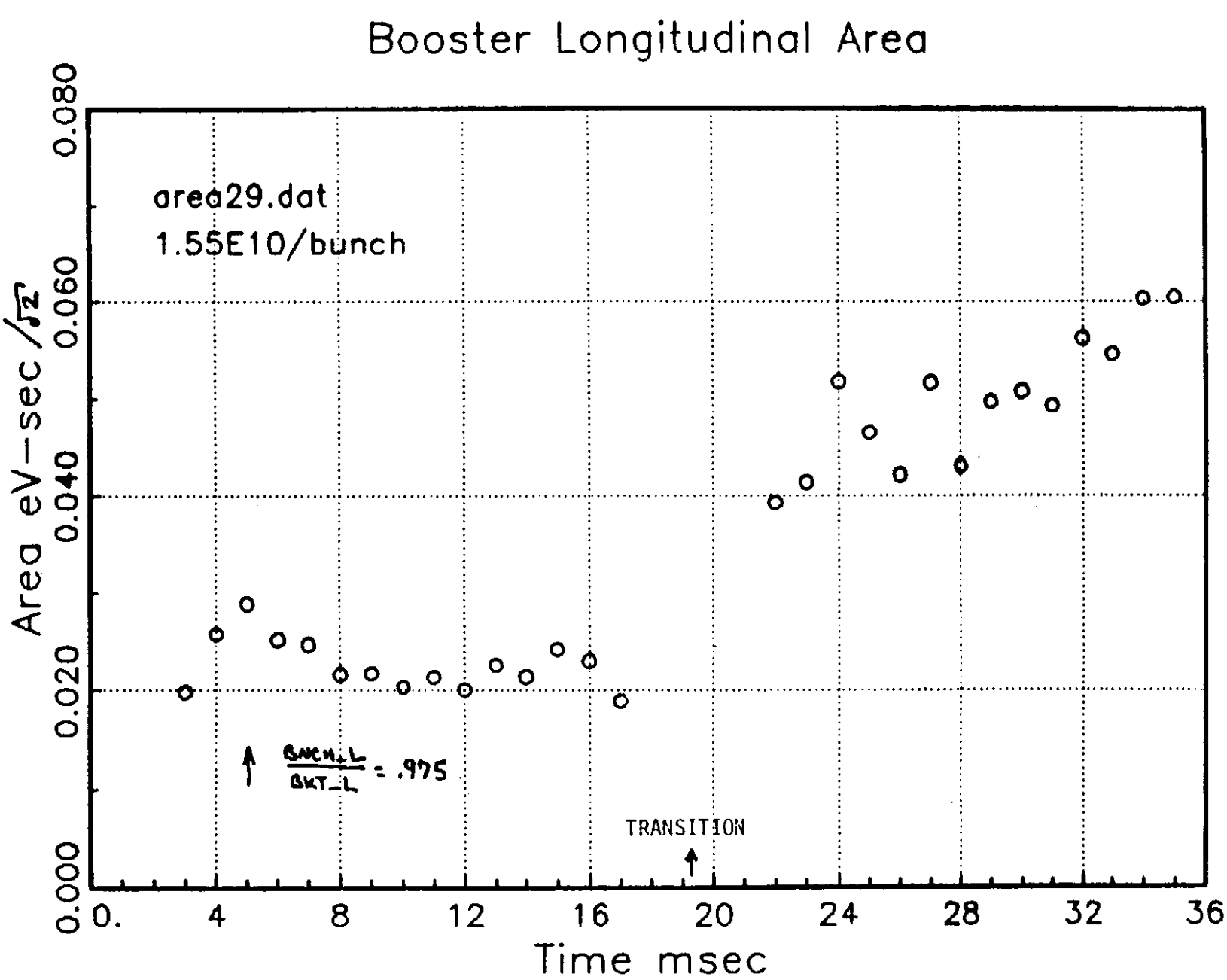

Figure 1: The bunch area of the Fermilab Booster increases after transition.

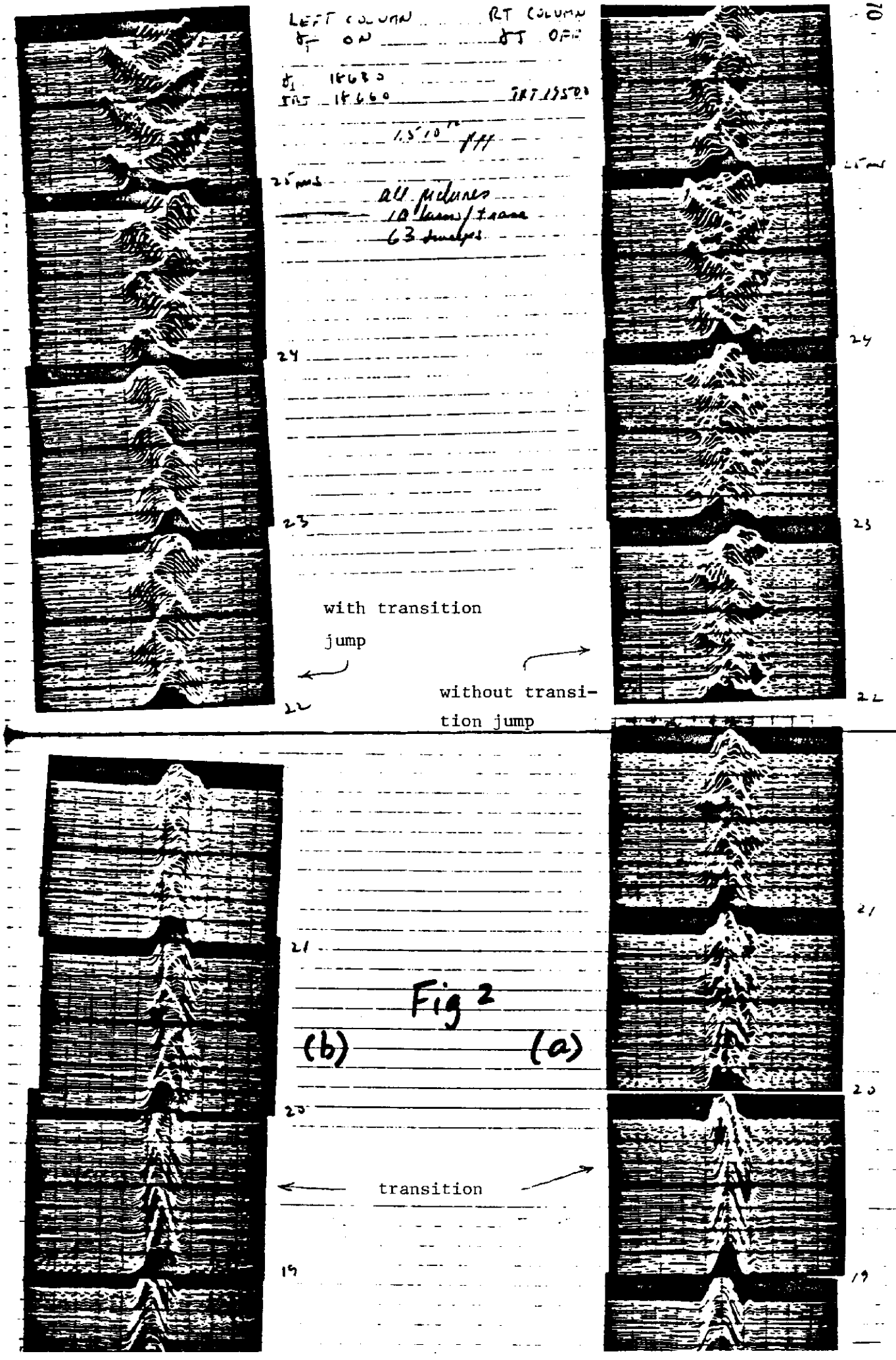
LEFT COLUMN
B_T ON
RT COLUMN
B_T OFF
B_1 16680
I_{BT} 16660
I_{BT} 13502
1.5×10^{22} n/cm²
25 msec
all pictures
10 turns/frame
63 shots
24
23
22
with transition
jump
without transition jump
21
20
19
transition
(b)
(a)

Fig 2

Figure 3: The difference in equilibrium bunch length before and after transition due to space-charge effects.

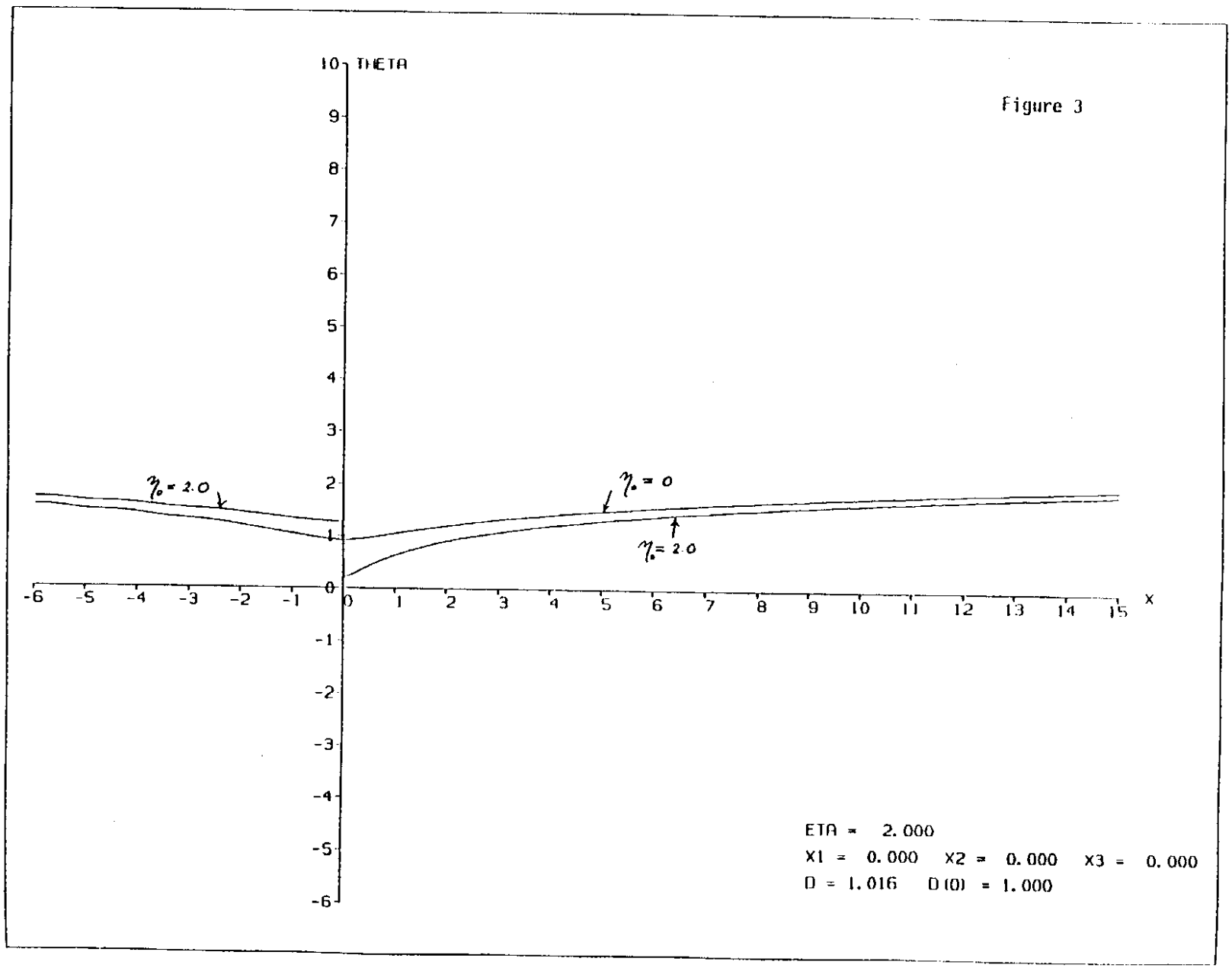

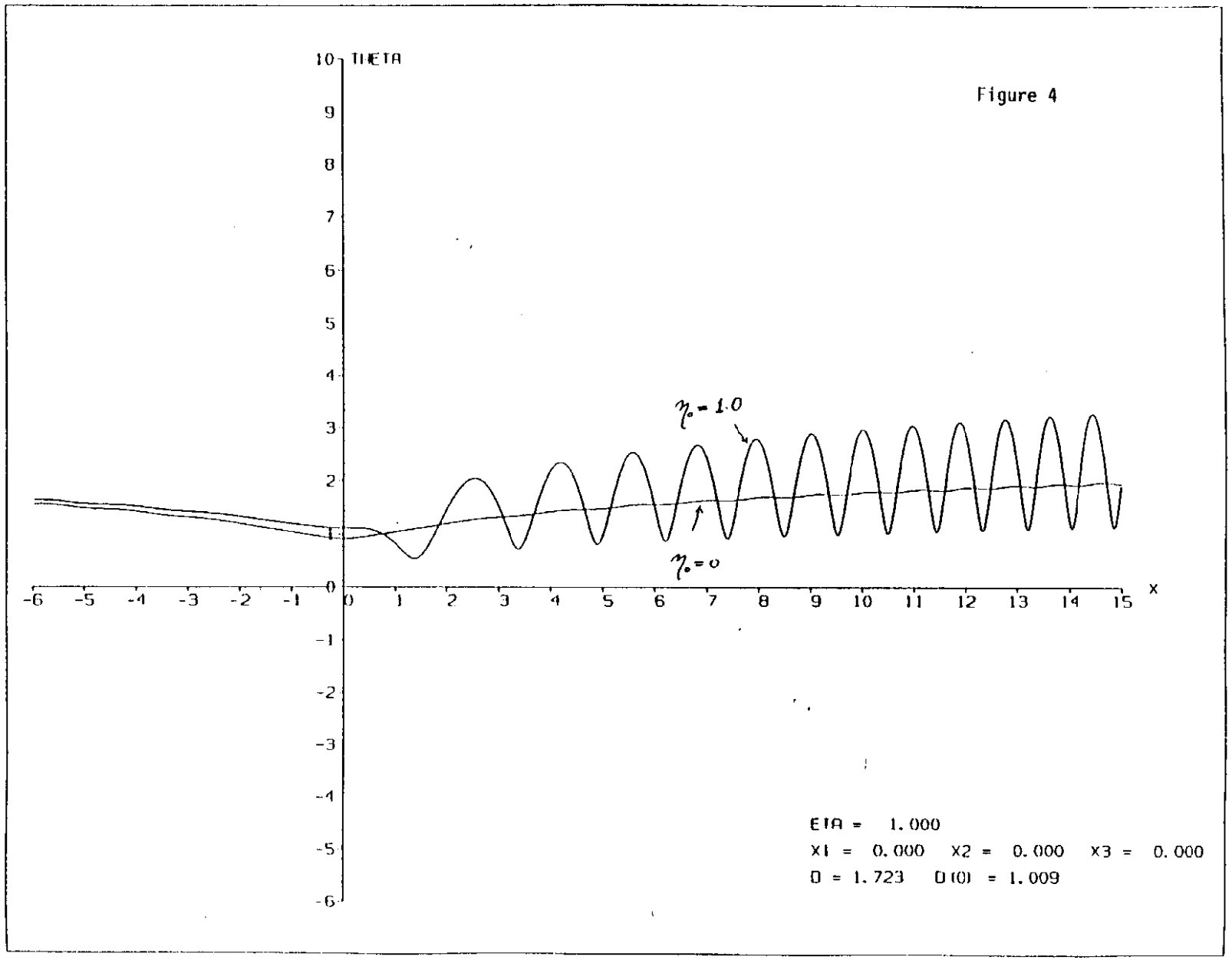

Figure 4: The tumbling of a bunch after crossing transition due to space-charge effects.

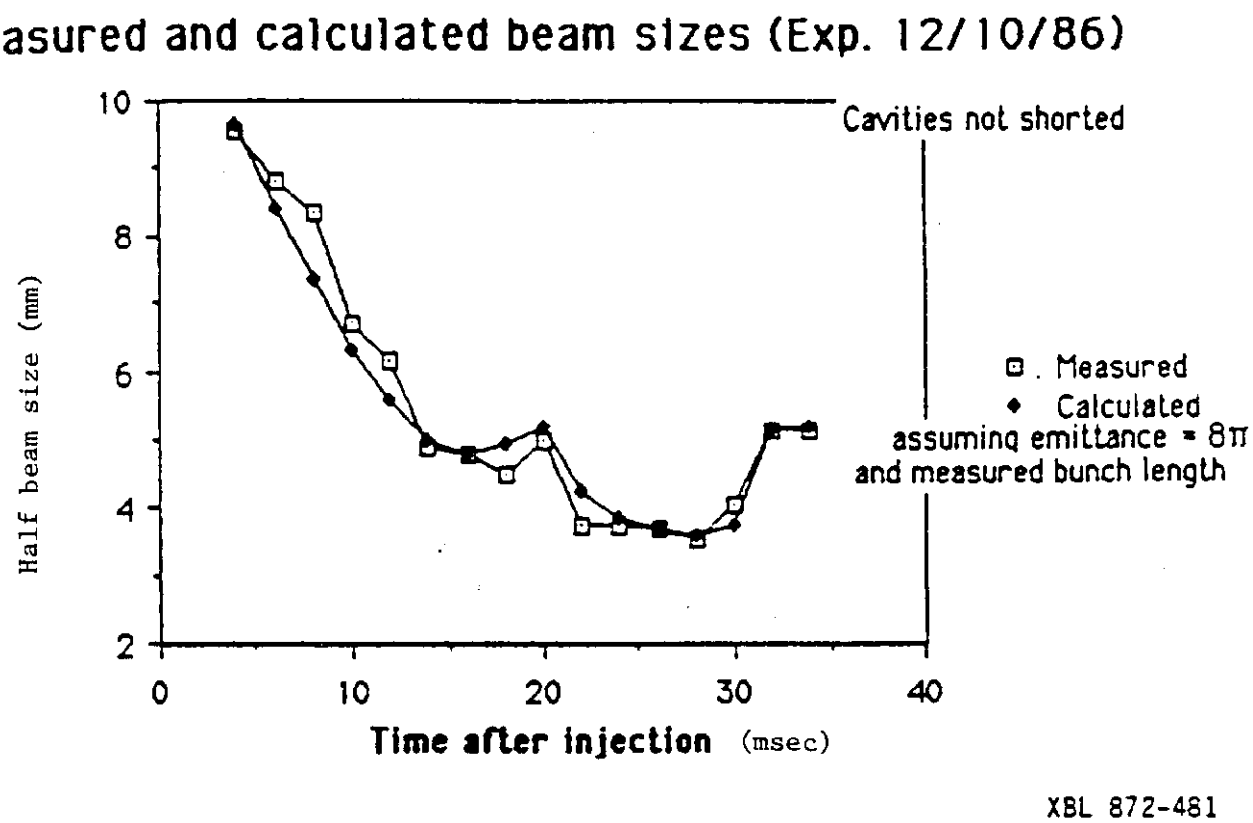

Fig. 5: Measured and calculated beam sizes at various times after injection. Four of the 18 cavities are off, but not shorted.

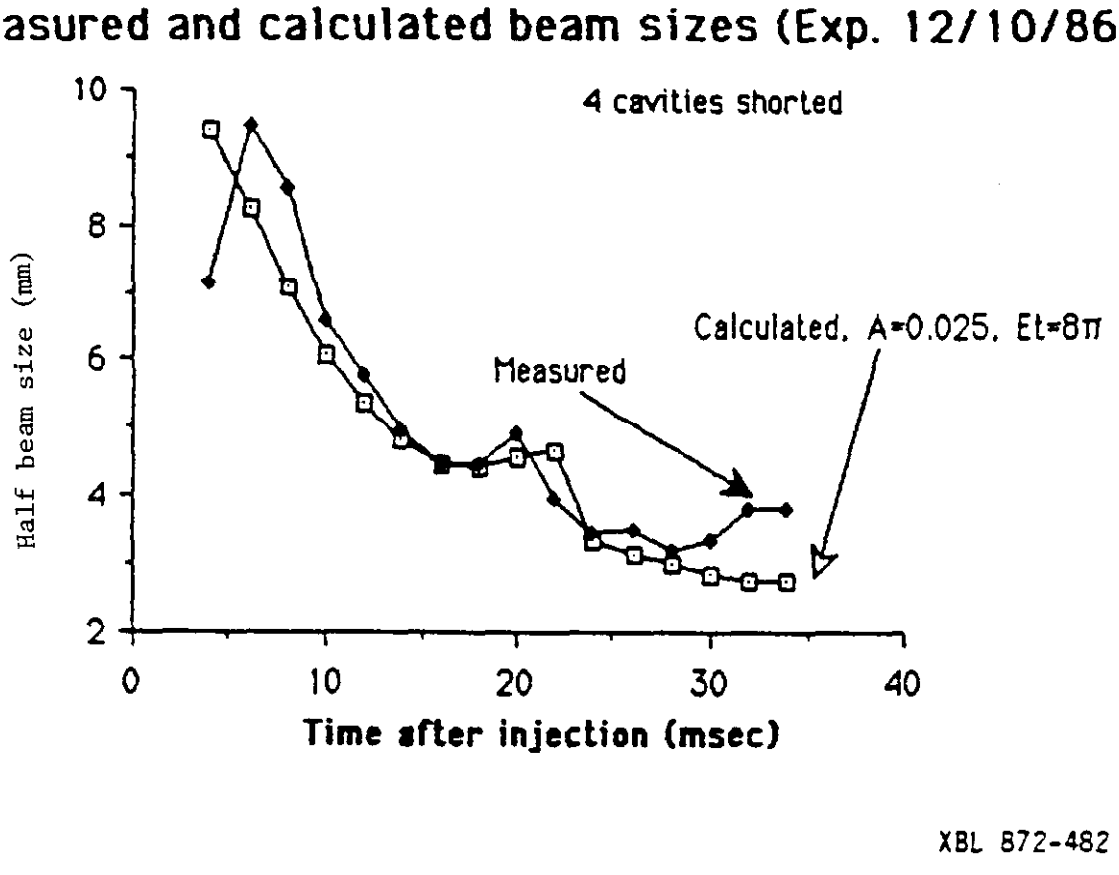

Fig. 6: Measured and calculated beam sizes with 4 cavities shorted.

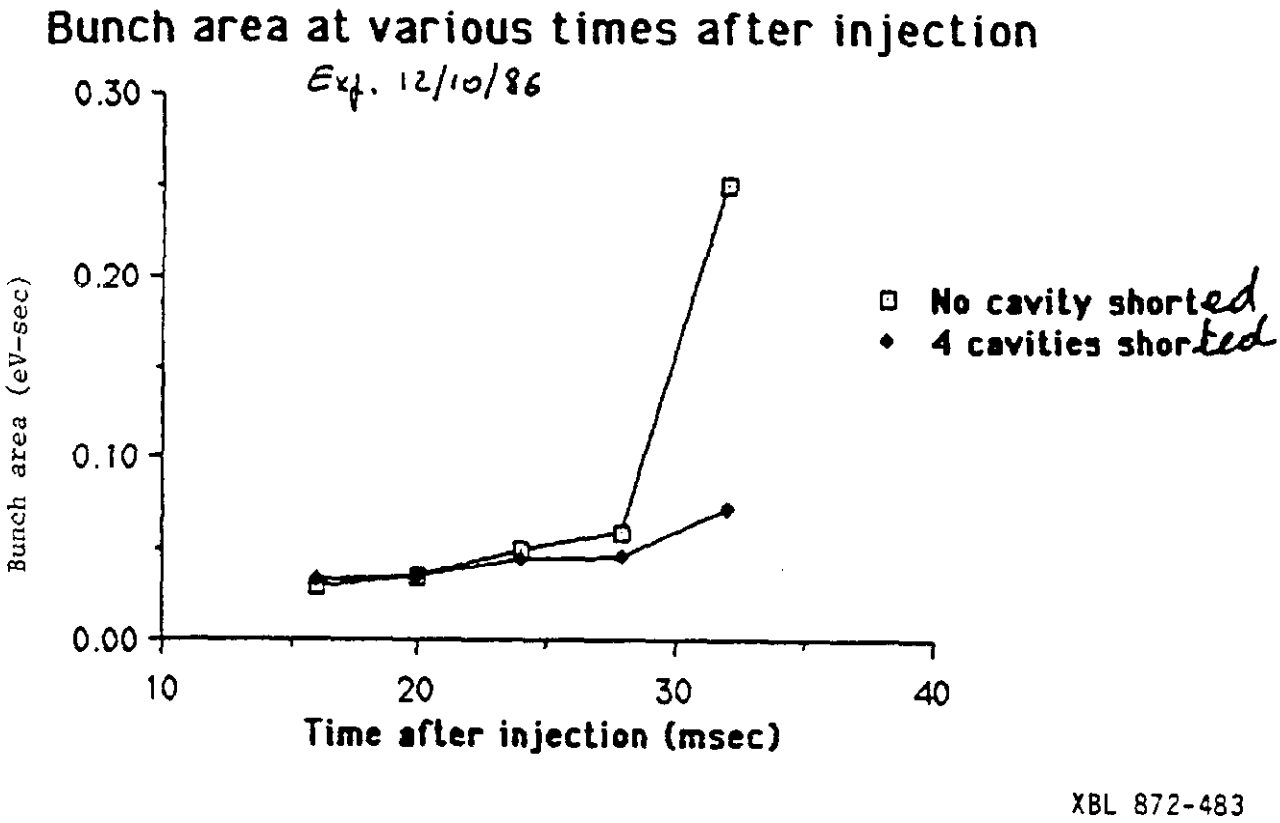

Fig. 7: Bunch area with shorted and unshorted cavities.

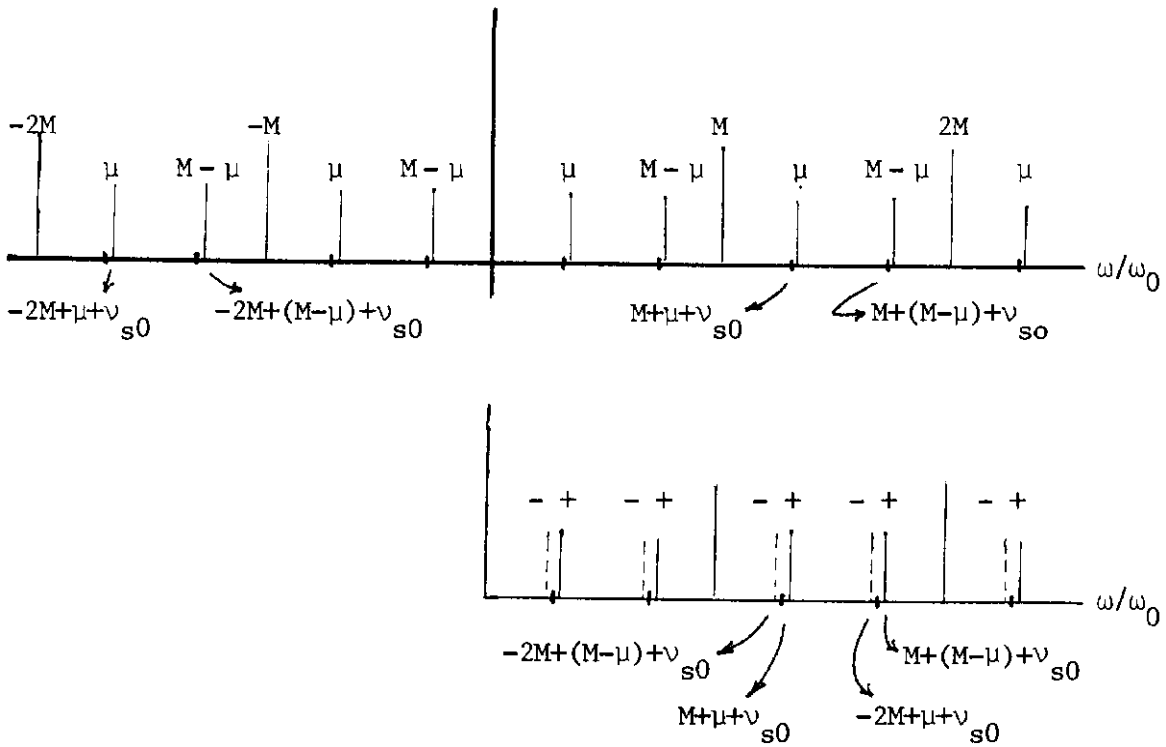

Figure 8: Spectral lines of coupled modes μ and M−μ. "+" represents positive-frequency line and will be excited as a growth, "−" represents negative-frequency line and will be excited as damping.

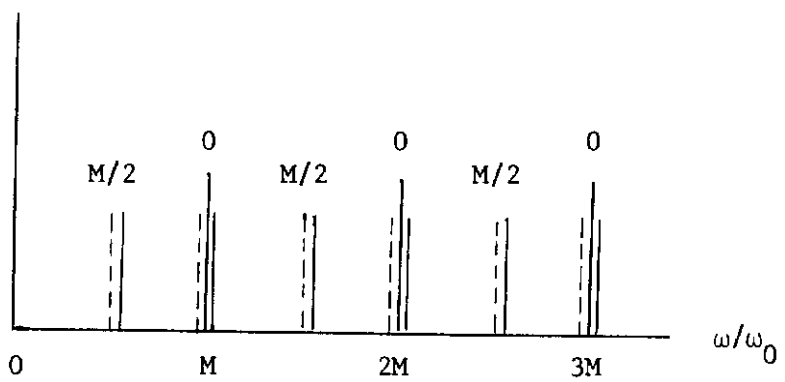

Figure 9: The positive (solid) and negative (dotted) frequency lines of modes μ = 0 and μ = M/2 (if M is even) are separated by $2\nu_{s0}\omega_0$ only. Thus, for a driving resonance that is wider than this, these two modes will be at least almost stable.

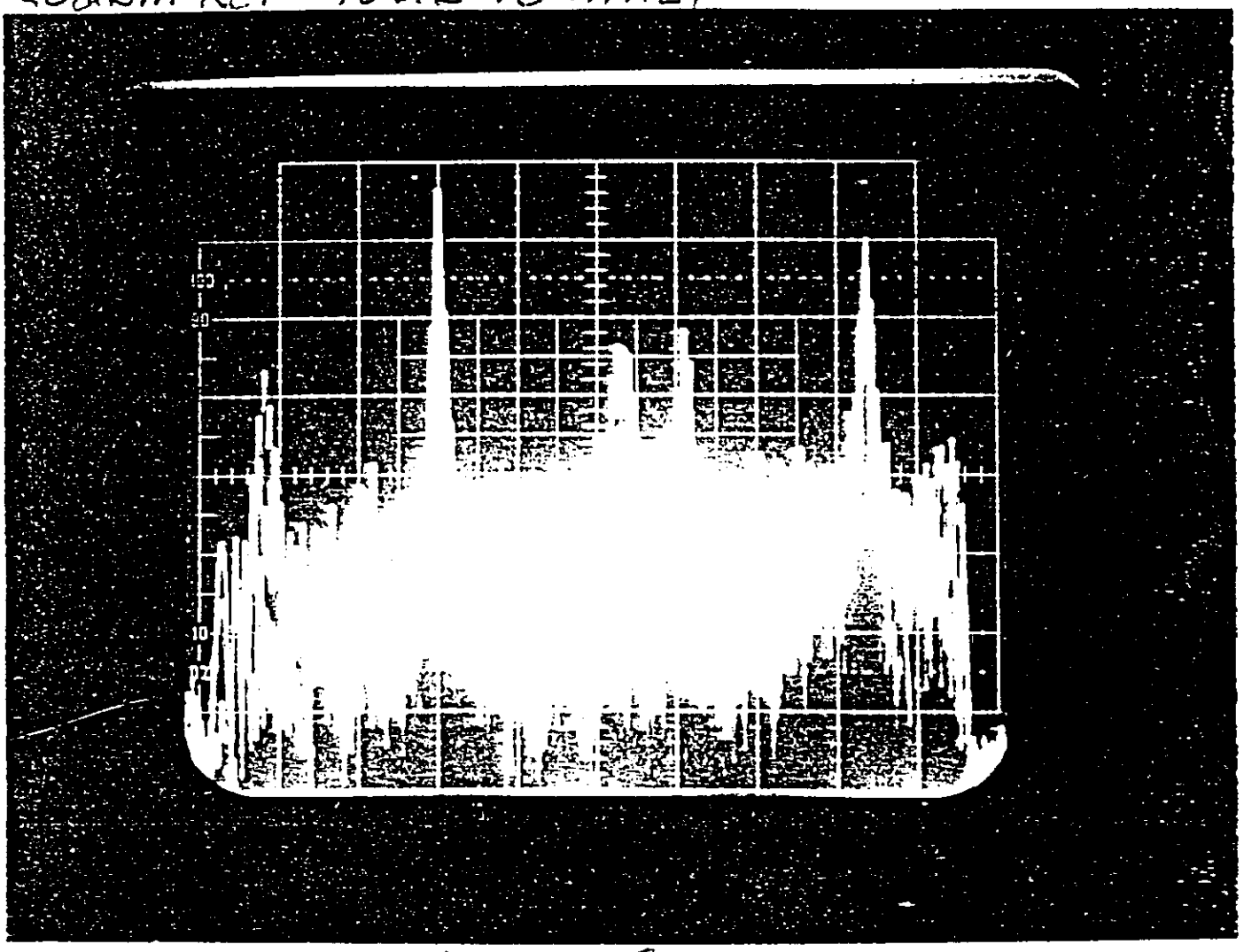

Figure 10: Beam spectrum of the booster showing the excitation of coupled-bunch mode 31 or 53.

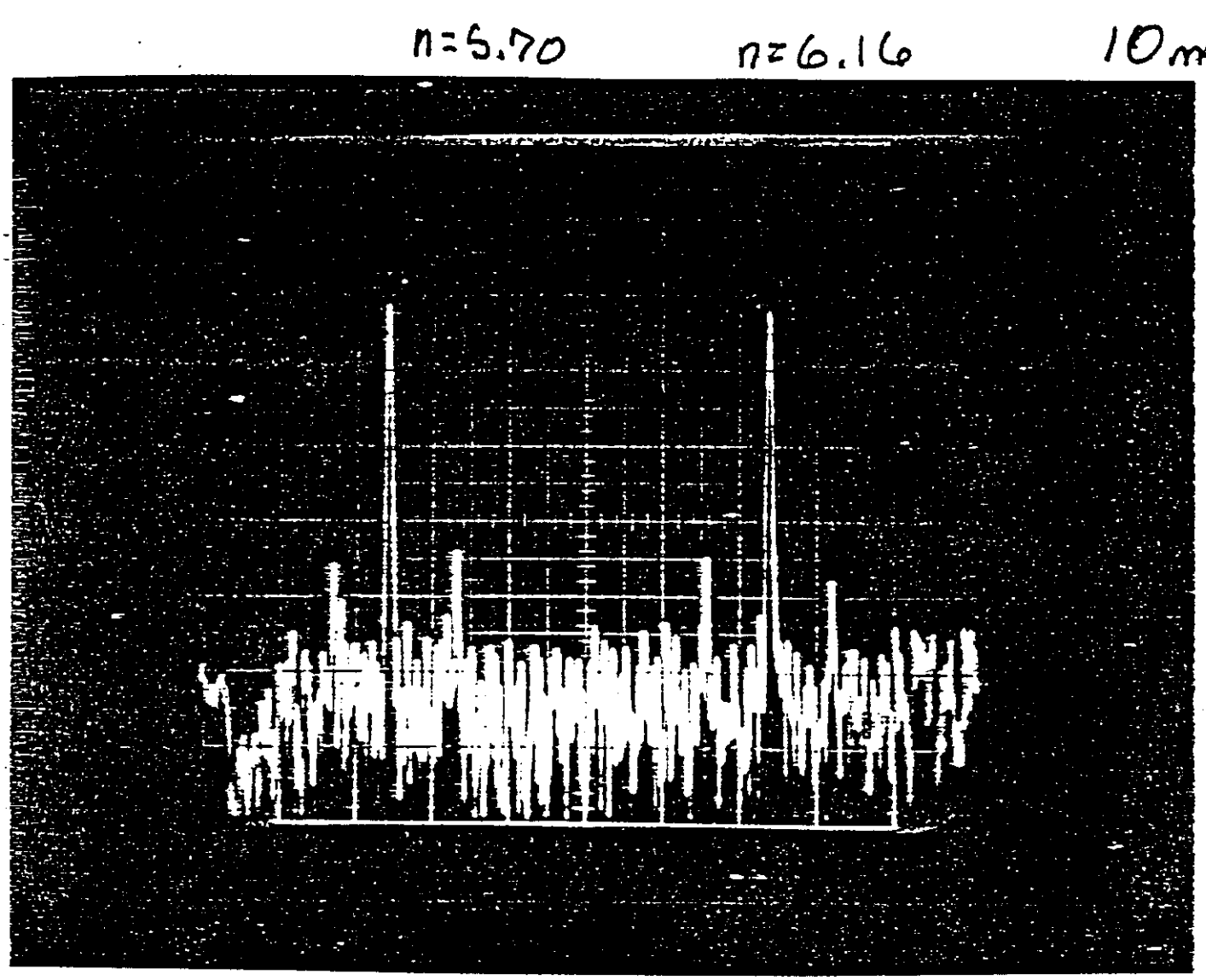

Figure 11: Beam spectrum of the booster showing the excitation of coupled-bunch mode 16 or 68.

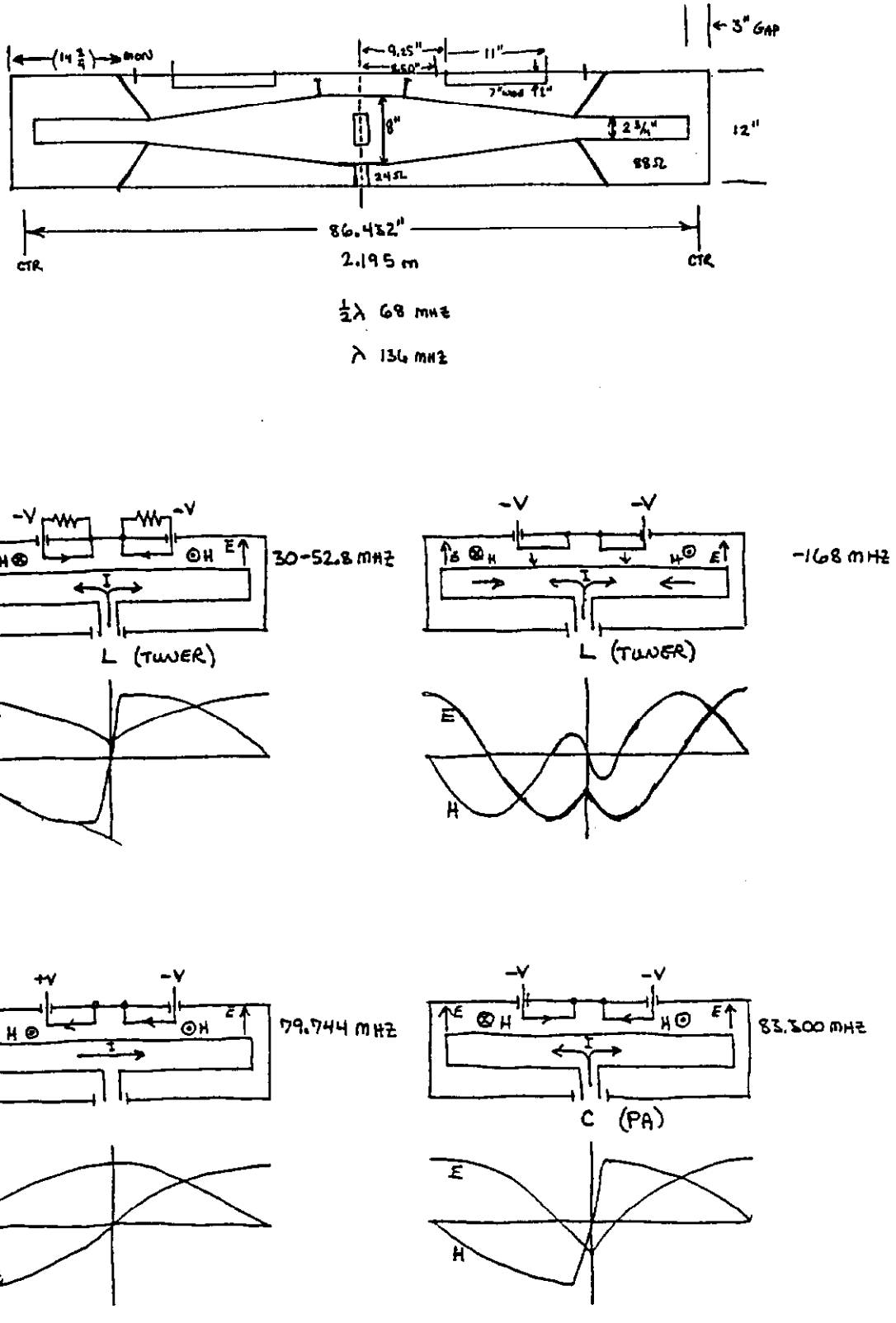

Figure 12: One rf cavity of the Fermilab Booster and the field structures of several resonance modes.

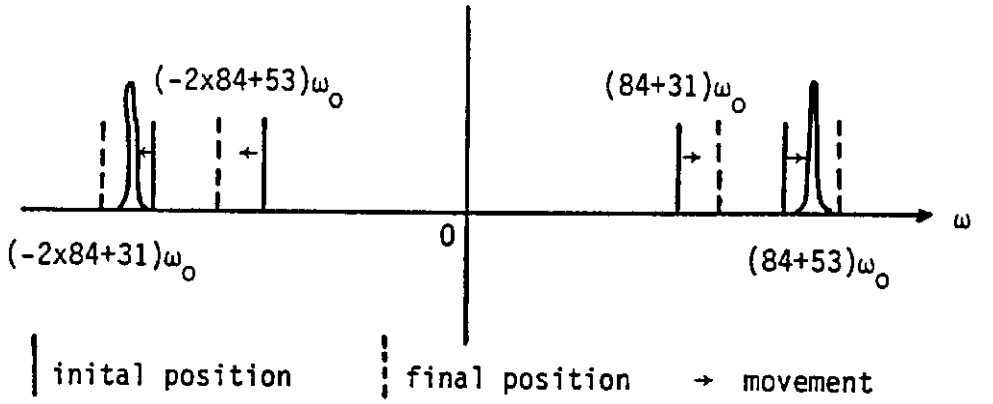

Figure 13a: The cancellation of growth by the insertion of a self-excited resonant cavity.

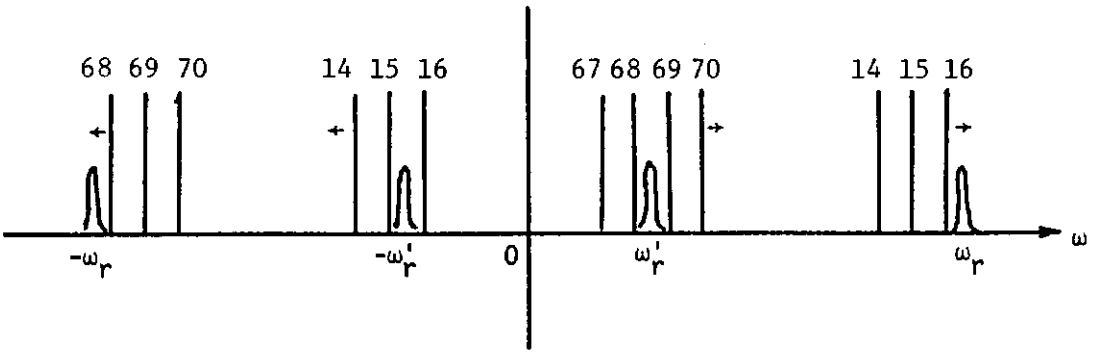

Figure 13b: A self-excited cavity will not work when the original resonance is crossed by spectral lines of several coupled-bunch modes.

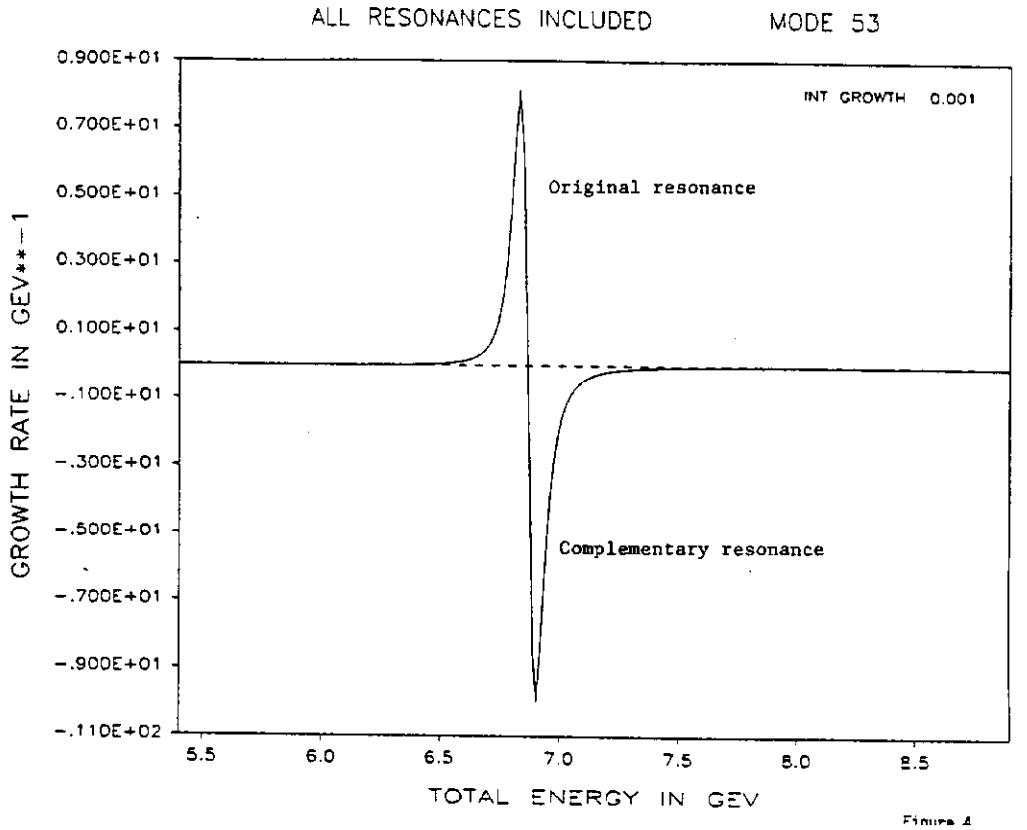

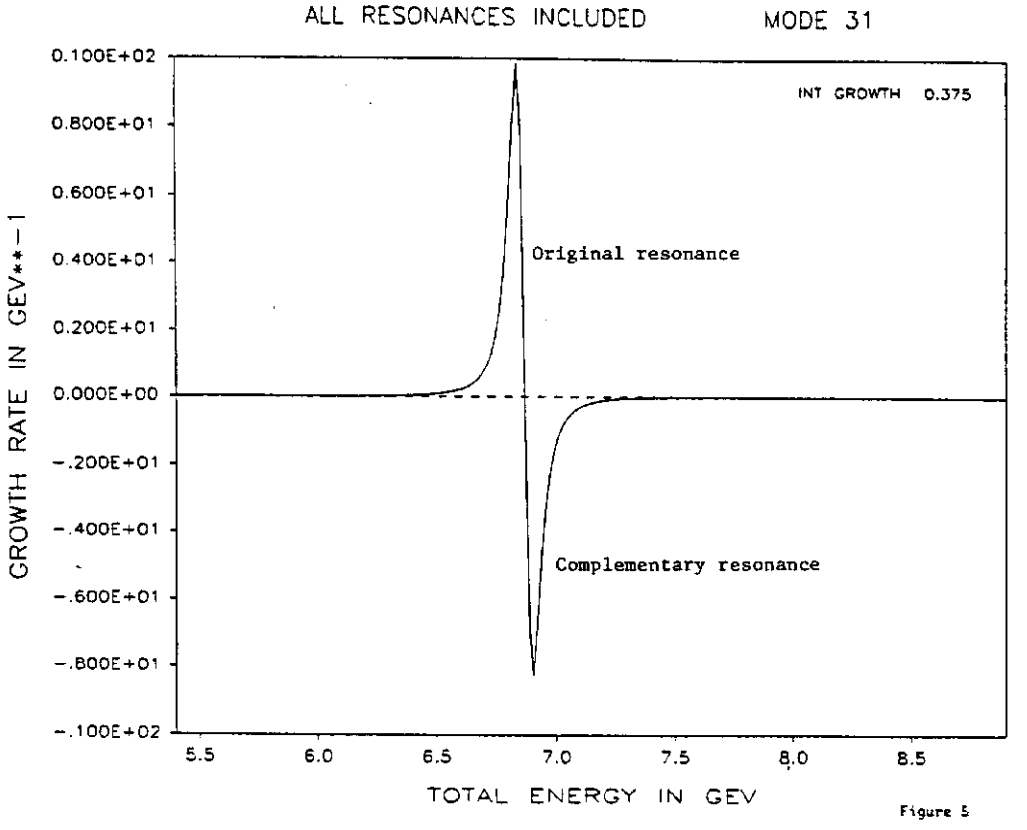

Figure 14: Graphs showing the growth immediately followed by damping for coupled-bunch mode 53 and 31 driven by resonance number 2 and a self-excited complementary cavity.

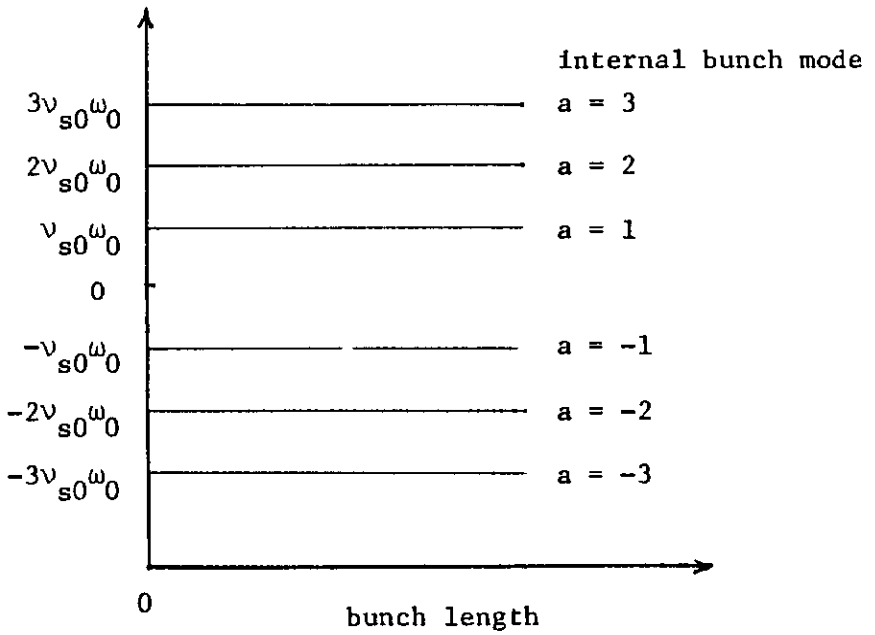

Figure 15: Internal bunch mode spectrum as a function of bunch length for a weak beam current.

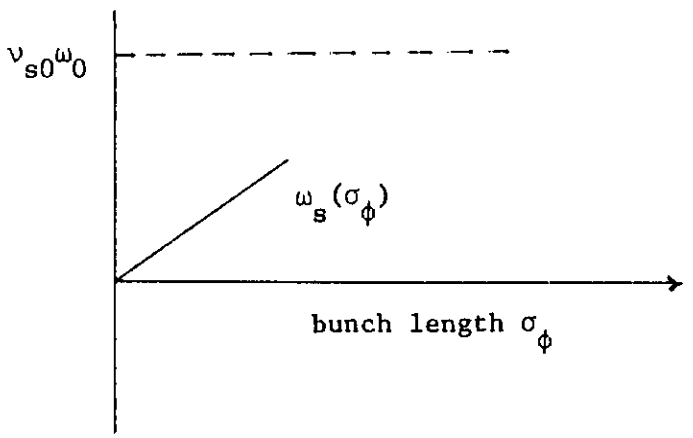

Figure 16: Internal bunch mode spectrum as a function of bunch length for a weak beam current.

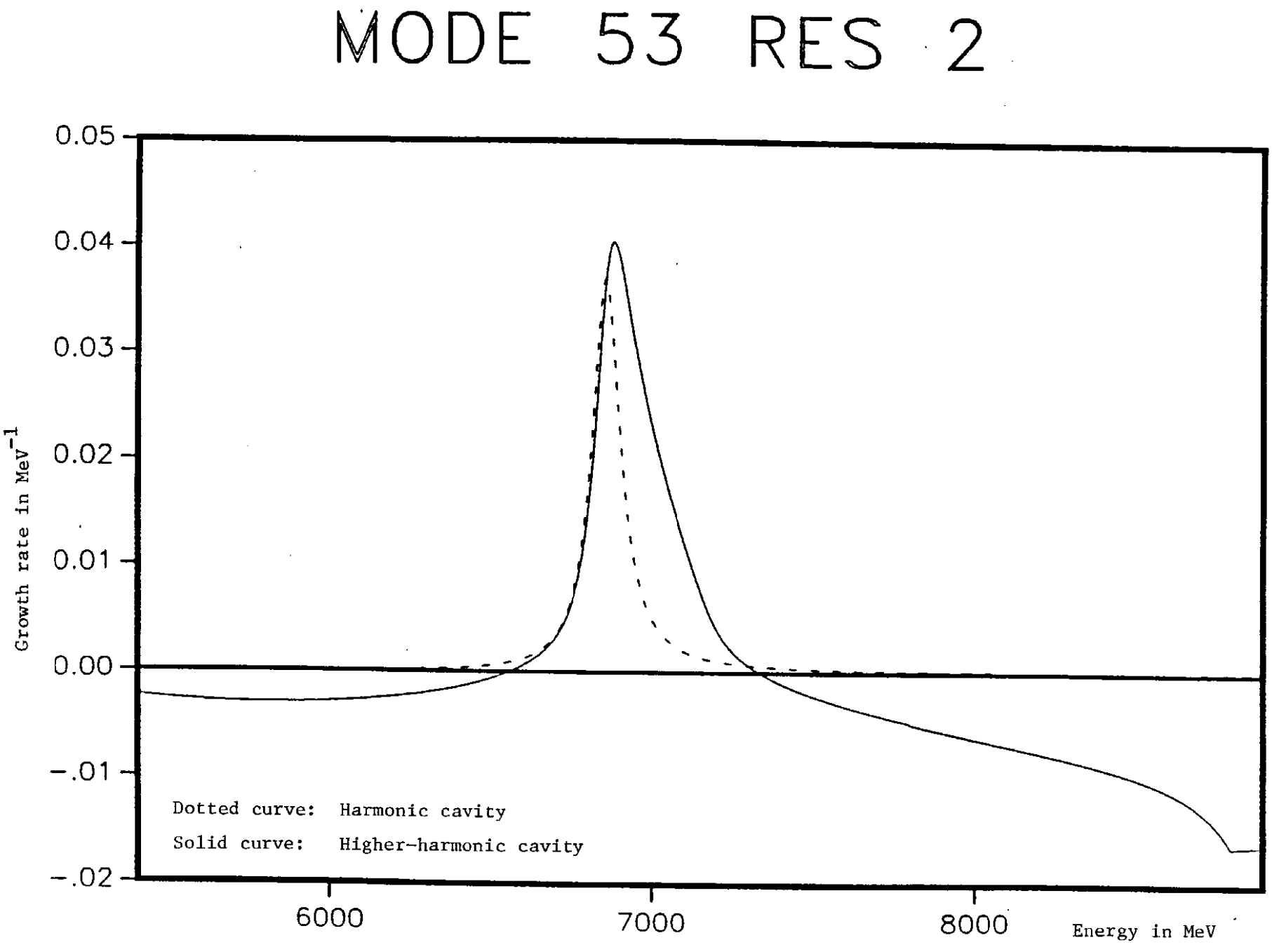

Figure 17: Growth rate for coupled-bunch mode 53 driven by resonance number 2.

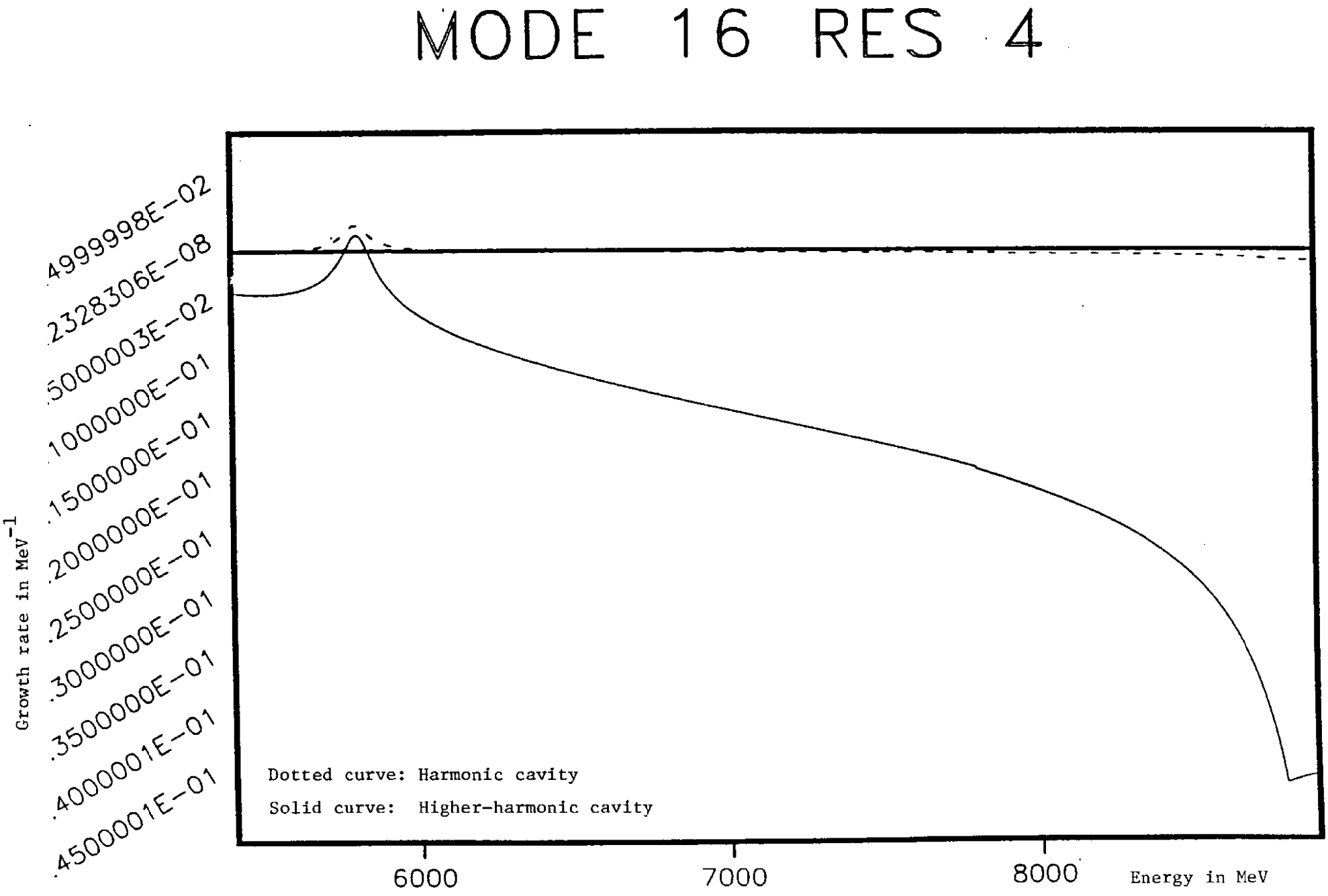

Figur 18: Growth rate for mode 16 driven by resonance number 4.